J. Agr. Sci. Tech. (2022) Vol. 24(4): 885-900

Investigation of Antioxidant, Antimicrobial and Anticancer Potential of Silver Nanoparticles Synthesized by *Viola tricolor* L. Extract

A. Hassanvand[1], S. Saadatmand[1*], H. Lari Yazdi[2], and A. Iranbakhsh[1]

ABSTRACT

Silver Nanoparticles (AgNPs) are widely used in medical and pharmaceutical applications due to their antimicrobial properties. In this study, Ag-NPs were synthesized using *Viola tricolor* aqueous extract as a reducing and capping agent. The presence of synthesized Ag-NPs was first confirmed with UV-Visible, SEM, TEM, XRD, and FTIR analyses, and then their antimicrobial characteristics were studied based on the Minimum Inhibitory Concentration (MIC). The SEM analysis showed that the synthesized AgNPs were spherical in shape. The particle size histogram revealed that the average particle size of the AgNPs was 49.45 nm. Findings from the FTIR and UV-Vis spectra showed the successful formation of Ag-NPs because the functional groups involved in the synthesis process and adsorption peaks were well developed. Furthermore, the Ag-NPs had a peak absorption at 420 nm in the spectrometry. MIC results showed the strong antimicrobial effects of the synthesized Ag-NPs. Results of the Minimum Bactericidal Concentration (MBC) revealed the dose-dependent cytotoxicity of the Ag-NPs. Nanoparticles could exert the inhibitory effect of DDPH free radicals in a dose-dependent manner. Methyl Tetrazolium (MTT) results showed that silver nanoparticles had a dose-dependent cytotoxic effect and significantly reduced cell survival. The IC50 values for Ag-NPs and the extract were 11.83 and 204.4 µg mL^{-1}, respectively. This study showed a higher cytotoxic effect of the green synthesized nanoparticles on hepatocellular carcinoma cells than the extract. Consequently, the biosynthesis of Ag-NPs using aqueous extract of *V. tricolor* is clean, inexpensive, and has antibacterial, anticancer and antioxidant activities. Hence, it can be used as a drug candidate.

Keywords: Antimicrobial characteristics, Cytotoxicity, Minimum bactericidal concentration Minimum inhibitory concentration.

INTRODUCTION

Nanotechnology deals with controlled manipulation of the molecular and atomic structures of substances from 1 to 100 nm size, which shows unique mechanical, thermal, chemical, and magnetic properties (Agarwal *et al*., 2018). Generally, metal nanoparticles are synthesized from mineral metals using several chemical methods, including microemulsion, radiation reduction, chemical reduction, electrochemical reduction, and radiation (Jagtap *et al*., 2013). The drawbacks of these methods include hazards to human health and the environment as well as the high cost of reducers. Recently, a number of affordable and high-yield biological methods have been developed for the synthesis of silver Nanoparticles (AgNPs). Using microorganisms or plant extracts may substitute the chemical methods used for the mass production of metal or metal oxide nanoparticles (Gan *et al*., 2012).

Among the metal nanoparticles, Ag-NPs

[1] Department of Biology, Science and Research Branch, Islamic Azad University, Tehran, Islamic Republic of Iran.
[2] Department of Biology, Borujerd Branch, Islamic Azad University, Borujerd, Islamic Republic of Iran.
*Corresponding author; e-mail: sadatmandsara@gmail.com

have attracted special attention due to their strong antimicrobial effects. Ag-NPs are highly important for medical usages (antibacterial dressings, dental substances, sunscreen lotions, tracheal tubes, urinary catheters, etc.), the textile industry, and water refinery due to their antibacterial properties. The function of Ag-NPs is affected by their size, shape, concentration, and chemical composition(Chand *et al*., 2019). Given their high surface-to-volume ratio, the antibacterial effect of Ag-NPs is very superior to silver particles. Ag-NPs damage the cellular membrane and inhibit bacterial DNA replication and free radicals or reactive oxygen species(Rashid *et al*., 2016).

Antibacterial action of Ag-NPs is mediated by several generally accepted mechanisms (depicted in Figure 1). The three most important routes of antimicrobial action of AgNPs are as follows: 1) Accumulation and disruption of the extracellular polymers of the bacterial biofilm; silver ions (Ag+) could also biochemically alter the biofilm overall adherence, structure, and porosity; 2) AgNPs adhere to bacterial cell surface resulting in microbial membrane disruption, altered transmembranar transport, cellular content leakage, and bacterial death, and 3) Ag-NPs penetrate bacterial cell wall and access microbial cytoplasm, where they can interact with the organelles, cytosolic molecules (as free amino acids, peptides, and enzymes) and bacterial cytoskeleton. The direct action of Ag-NPs and Ag+ results in alteration of several metabolic pathways, bacterial organelles dysfunction (mainly mitochondria), ROS generation and bacterial DNA alteration, ultimately causing cell death (Tăbăran *et al*., 2020) .

Nanoparticles may be synthesized using green synthesis methods, also known as the biocompatible methods (Ravichandran *et al*., 2019), in which plant extracts are used due

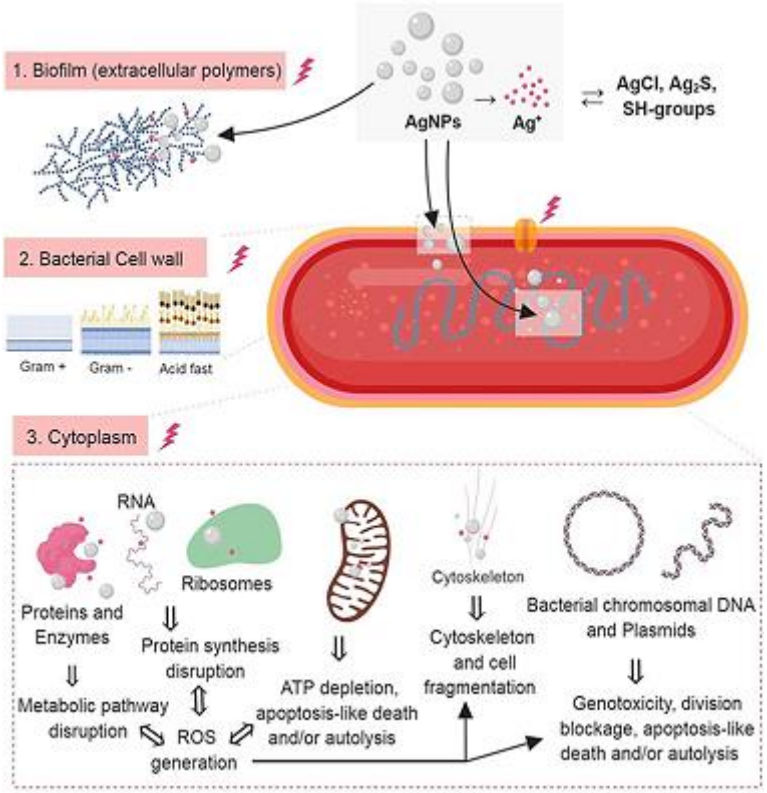

Figure 1. Schematic representation of the known mechanism(s) of antibacterial action of Ag-NPs and released ionic silver (Tăbăran *et al*., 2020).

to the presence of different metabolites, such as emulsifiers and fixators for the synthesis of nanoparticles, and are less costly and biocompatible, with a high yield. Moreover, plants are appropriate choices for the synthesis of nanoparticles since they do not require special growth conditions and special nourishments. Moreover, they contain terpenes, flavonoids, ketones, aldehydes, amides, and carboxylic acids, which directly reduce the ions and form Ag-NPs (Chand *et al*., 2020). Today, several plants, including *Abutilon indum, Erythrina indica, Ocimum tenuiflorum, Melia dubia, Ziziphora tenuior, Acalypha indic*, and *Solanum tricobatum*, are used in the synthesis of Ag-NPs using green synthesis methods, as these plants could reduce silver ions in very small sizes. Different plant organs, such as leaves, roots, flowers, fruits, and seeds, may be used depending on the type of nanoproducts (Ruttkay-Nedecky *et al*., 2017). In a study by Rashid *et al.* (2016), the extract of *Artemisia marschalliana* Sprengel (sagebrush) with strong reducing compounds was used for the synthesis of Ag-NPs (Patra *et al*., 2016).

As a major species of the genus Viola, *Viola tricolor* L. is a traditional plant belonging to the Violaceae family. It has long been used in Europe for the treatment of various diseases, including pulmonary inflammatory disease, inflammatory skin disorders, epilepsy, dyspnea, rheumatism, and asthma. This plant is rich in mucilage, flavonoids such as rutin, violantin, violaxanthin, violaquercetin, anthocyanidin glycosides, and some saponins, ascorbic acid, alpha-tocopherol, alkaloids, and essential oils, with considerable antioxidant activity (Ebrahimzadeh *et al*., 2010).

Many plants of the Violaceae family have been used in traditional remedies, and these plants contain several cyclotide compounds with strong cytotoxic effects In general, bioactive plant cyclopeptides are interesting candidates for drug development. Cyclotides have a range of interesting bioactivities, including uterotonic, anti-HIV, anti-fungal, cytotoxic, anti-bacterial, nematocidal, molluscicidal, hemolytic, neurotensin antagonistic, insecticidal, and trypsin inhibitory activities. (Tang *et al*., 2010)

Due to their reducing role in the biosynthetic process of Ag-NPs and the important role of flavonoids in the extract of *V. tricolor*, this study aimed to evaluate the high potential of the extract of *V.tricolor* in the biosynthesis of silver nanoparticle and investigate the crystallographic structure and size of the synthesized Ag-NPs, and the effects of these nanoparticles on hepatocellular carcinoma and some bacterial strains.

MATERIALS AND METHODS

Collection, Identification, Storage, and Extraction Methods

The wild species of *V. tricolor* were supplied from the Agricultural Jihad Research Center of Lorestan Province, Iran. Flowers of the plant were first washed with distilled water, dried in the airflow, powdered using an electric mill, and then stored in glass vessels. To prepare the extract, 10 g of the flower powder was added to 100 mL of distilled water and then placed in a Ben Marie device (at 70°C for 45 minutes). The prepared aqueous solution was cooled, passed through Whatman filter papers, and stored at 4°C until the synthesis of AgNPs.

Preparation of Silver Nanoparticles

Silver nitrate was used as a precursor for the synthesis of Ag-NPs by adding 40 mL of *V.tricolor* flower (10 g) extract to 10 mL of 0.1 M silver nitrate solution at room temperature. The solution was placed on a magnetic stirrer for 24 hours and then centrifuged at 14,000 rpm for 15 minutes. The formation of NPs resulting from $AgNO_3$ reduction was monitored by observation of the color change (the color of the samples changed from reddish to grey) in the mixture

after the overnight incubation at room temperature. The nanoparticle precipitate was washed using sterile distilled water to remove contaminants and, finally, the precipitate was dried at room temperature (Chand *et al*., 2020).

Characterisation of Silver Nanoparticles

UV-Vis Spectrometry Analysis

Two hours after adding the extract to silver nitrate and changing the solution color, Ag-NPs were analyzed using a UV-Vis spectrometer (Agilent, Spectrophotometer, USA) at wavelengths of 200-700 nm. Figure 2 shows the UV-Vis spectral characteristics of the plant extract, silver nitrate solution, and the mixture of the plant extract with silver nitrate. The difference in the spectrum curves can be attributed to the stimulation of plasmon surface vibrations due to the presence of silver nitrate in the reaction mixture(Mousavi *et al*., 2018).

EDX, SEM, TEM and XRD Analyses

To evaluate the properties of the synthesized nanoparticles using aqueous extract of Pansy, various analysis techniques including, scanning electron microscope (Model QUANTA 200, USA), and transmission electron microscopy (Model CM10 made by PHILIPS Germany) were used. Preliminary analyses of Ag-NPs were performed using an X-ray Energy scattering Detector (EDX) (Model VEGA3.Tescan) (Ravichandran *et al*., 2019). XRD (Philips X'PERT PROMPD) measurements were performed on an advanced BrukerD8 instrument using Cu Kα anode (λ= 0.1542 nm) with a voltage of 45kV and a current of 40 mA on a glass slide coated with a drop of nanoparticle solution.

FTIR Analysis

Fourier Transform Infrared (FTIR) spectroscopy was carried out for predicting responsible groups for NPs synthesis and stabilization. FTIR was used to identify the functional groups of potential biomolecules (responsible for reducing silver ions and the agents covering Ag-NPs). Infrared (IR) spectra of the samples were recorded using the FTIR (FTIR Perkin Elmer Model 10.02.00) device.

Evaluation of Antimicrobial Activity

The antibacterial and antifungal activities of Ag-NPs were investigated by the agar well diffusion method. Standard and clinical microbial strains of Gram-positive and

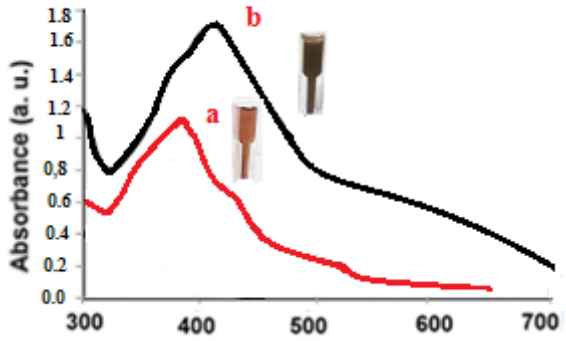

Figure 2. UV–Vis spectra of AgNPs: (a) *V. tricolor* extract, and (b) Ag-NPs solution.

Gram-negative bacteria, such as *Escherichia coli* (PTCC1330), *Staphylococcus aureus* (PTCC 1112), *Pseudomonas aeruginosa* (PTCC 1074), *Salmonella typhi* (PTCC 1639), *Staphylococcus saprophyticus* (ATCC 15305), *Bacillus cereus* (PTCC1556), *Klebsiella pneumoniae* (PTCC 1053), *Candida albicans*, and *Candida glabrata*, were obtained from the Iranian Research Organization for Science and Technology (IROST). Then, 100 µL of each microbial suspension (5.5 McFarland) was poured on a plate containing Müller Hinton Agar (MHA) for bacteria and Sabouraud Dextrose Agar (SDA) for fungi and cultured in three directions with sterile swabs. Using a sterile Pasteur pipette used for making wells, five holes with an approximate diameter of 7 mm and a distance of 2 cm were made on the surface of each cultured plate, and 1 mL of each prepared dilution of Ag-NPs was poured at different concentrations (100, 500, and 1,000 µg mL^{-1}) in each well with a sampler. Amikacin, an antibacterial antibiotic, and amphotericin B, an antifungal agent, were used as positive controls. Different concentrations of Ag-NPs in wells 1, 2, and 3, plant extract in well 4, and amikacin or amphotericin B in well 5 were used as positive controls. Then, bacterial culture media were incubated at 37°C for 24 hours, and fungal culture media were incubated at 28°C for 48 hours. This operation was repeated four times for all four samples, and then the diameter of the impermeability hallo was calculated in millimeters (Keshari *et al*., 2020).

Minimum Inhibitory Concentration (MIC) and Minimum Bactericidal Concentration (MBC)

MIC was determined using the micro-dilution method according to guidelines of the Clinical and Laboratory Standards Institute (CLSI). Different dilutions were prepared from Ag-NPs solutions to achieve different concentrations. One mL of each dilution was added to 4 mL of Müller Hinton Broth (MHB) in sterile vials. Freshly cultured cells (100 µL) were inoculated into each tube at a light density of 0.5 McFarland. The test and control (no treatment) tubes were incubated at 37°C for 24 hours. Then, 100 µL from all tubes was spread on plates containing agar medium by a Pasteur pipette, and the plates were incubated at 37°C for 24 hours. Next, bacterial growth was determined by measuring light density at 600 nm using a UV-Vis spectrophotometer. The plate containing a maximum of 10 tested bacterial colonies was considered as the MIC and the plate with no bacterial growth was assigned as the MBC. To determine the MBC, the tubes with no bacterial growth were cultured on MHA sheets and incubated at 37°C for 24 hours (Gilavand *et al*., 2020).

Antioxidant Capacity of Silver Nanoparticles

The antioxidant capacity of Ag-NPs was measured using the DPPH method to evaluate free radical scavenging activity (Bhakya *et al*., 2016). First, different concentrations of Ag-NPs (6.25, 12.5, 25, 50, and 100 µg mL^{-1}) were mixed with 600 µL of 0.1 mM DPPH in a small test tube and incubated at room temperature in a dark place for 30 minutes. Afterward, the absorbance was measured by a spectrometer at a wavelength of 720 nm. Butylated Hydroxyanisole (BHA) was used as a positive control and ethanol as a blank. The following equation was used to calculate the degree of inhibition:

$$A\ (\%) = 100 \times [(A_{control} - A_{sample} / (A_{control})] \quad (1)$$

where $A_{control}$ is the absorbance of the control and A_{sample} is the absorbance of the AgNPs.

Anticancer Activity of Silver Nanoparticles

In this study, hepatocellular cell lines were obtained from the cell bank of Pasteur Institute of Iran and incubated in RPMI-

1640 culture medium with 10% fetal bovine serum, 1% antibiotic, and 2 mM of L-glutamine at 37°C with 5% CO_2. Next, the MTT colorimetric method was used to investigate the effects of AgNPs and the extract on the growth and proliferation of cells. At first, 200 µL of a prepared cell suspension from the cancer cell line and different concentrations of AgNPs and the extract were added to each well. After 24 hours of incubation, 20 µL of MTT dye with a concentration of 5 mg mL^{-1} was added to each well of a 96-well plate, followed by incubation for 4 hours. Then, the contents of the wells were carefully drained and substituted with 50 µL of Dimethyl Sulfoxide (DMSO). To ensure that dye particles were dissolved after 30 minutes of incubation, the optical density of the wells was read at 570 nm using an ELISA reader. The concentration that inhibited cell growth up to 50% was considered the IC50 (Mousavi *et al*., 2018). The cell survival rate (%) was calculated using the following formula:

$$\text{Cell survival rate} = \left(\frac{\text{TreatedOD}}{\text{ControlOD}}\right) \times 100 \quad (2)$$

The experiment was performed as a completely randomized design with four replications. Data were analyzed statistically by SAS software, and means were compared using Duncan's test.

RESULTS AND DISCUSSION

Confirmation of Silver Nanoparticle Synthesis

AgNPs were synthesized by the green method by reducing silver ions using the extract of *V. tricolor*. The first sign that confirmed the biosynthesis of the nanoparticles was a gradual change in the color of the reaction solution. By adding *V. tricolor* extract to the silver nitrate solution, after a few minutes, the color of the samples changed from reddish to grey. This color change indicated the formation of silver nanoparticles. The first sign of silver nitrate reduction and the formation of Ag-NPs in the solution was the change of color. Using plants for the synthesis of Ag-NPs is cost-effective and has attracted significant attention to avoid use of harmful chemicals.

Plant extracts contain organic compounds, such as polyphenols, alkaloids, flavonoids, and anthocyanins, which have a powerful reducing function in the synthesis of Ag-NPs (Patra *et al*., 2016) and stabilize the nanostructures under reaction conditions. In this study, *V. tricolor* extract was used for the biosynthesis of Ag-NPs for the first time.

Figure 2 (a-b) shows the UV-Vis spectra of AgNPs and *V. tricolor* extract, respectively. As seen in Figure 2-b, a known adsorption signal at 420 nm is attributed to the formation of Ag-NPs. The maximum absorption peak of Surface Plasmon Resonance (SPR) of Ag-NPs in the obtained curve is seen between 400 and 450 nm. Continuous intensification of adsorption as a function of time indicates the reducing power of the extract. The color change and the difference in spectrum curves can be attributed to the stimulation of plasmon surface vibrations in the nanoparticles and the reduction of silver ions by the plant extract. The surface plasmon is caused by the excitation of cumulative charge fluctuations at the metal-dielectric interface. The results of this study are consistent with other studies. Keshari *et al* (2020) also proved that the resonant peak of Ag-NPs lies around this area.

Physicochemical Characteristics of Silver Nanoparticles

SEM, TEM and EDX Analysis

Microscopic techniques such as SEM and TEM were utilized to characterize the morphology of nanoparticles. The SEM analysis showed that the synthesized Ag-NPs were spherical in shape (Figure 3a). To obtain a better resolution, the Ag-NPs were scanned using TEM (Figure 3-b). The particle size histogram revealed that the

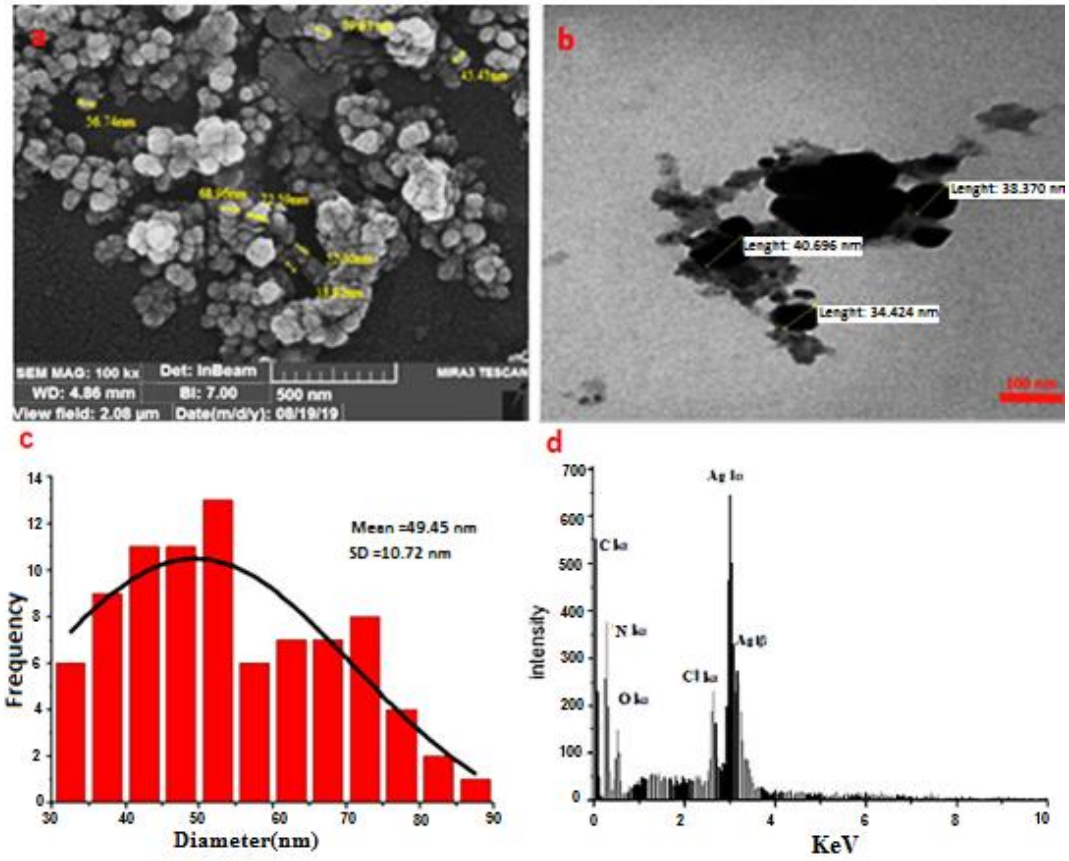

Figure 3. Electron microscopy analysis of biosynthesized Ag-NPs: (a) SEM micrograph, (b) TEM image, (c) A particle size distribution histogram from the SEM images, and (d) EDX spectrum**.**

mean size of the particle was 49.45 nm with 10.72 nm standard deviation (Figure 3-c). The size of nanoparticles ranged from 30 nm to 90 nm with maximum percentage of particles of 50–55 nm sizes, which was consistent with previous data (Poinern *et al*., 2013).

Comparison of the present study with other studies reveals that the size of the synthesized nanoparticles is affected by temperature, pH, duration of reaction, electrostatic force, concentrations of the saline solution, and plant extract interaction. Thus, according to the findings of Markus *et al*. (2017), the reaction occurs thanks to the interaction of concentrated silver nanoparticles with plant-derived organic compounds such as proteins and polysaccharides.

The quality and characteristics of the quantitative elements engaged in the synthesis of nanoparticles were determined using the EDX microanalysis. EDX analysis of the nanoparticles revealed that the most prominent peak appeared in 3.2kV, as well as a shoulder at 3.3kV. Strong signals at 3 KeV confirm the formation of the Ag-NPs in the solution (Figure 3-d). Signals of silver at 2-4 KeV in the biosynthesis of Ag-NPs using other plants have been reported by Ajitha *et al*.(2015) and Yuan *et al*.(2017). Other peaks like C and Cl may be assigned to X-ray emission from the biomolecules found in the violet flower aqueous extract (Khoshnamvand *et al*., 2019). The EDX spectrum reveals the relative silver (43.9%), carbon (35.8%), nitrogen, (13.83%) chlorine (4.72%) and oxygen (2.1%) contents.

XRD Analysis

Figure 4 shows the crystalline properties of Ag-NPs synthesized with *V. tricolor*

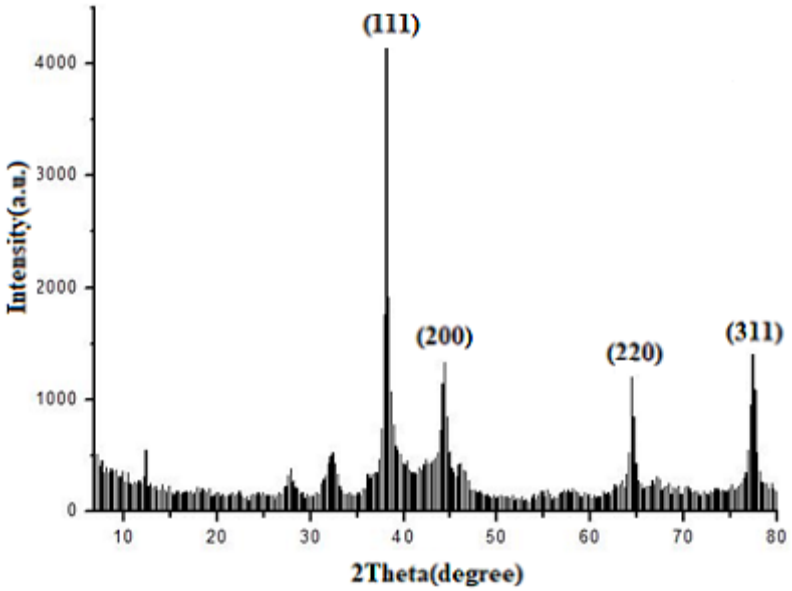

Figure 4. XRD images of Ag-NPs synthesized with *V. tricolor* extract.

extract and studied by XRD. Sharp peaks show the production of a highly crystalline material under the synthesis conditions, and the width of the strips infers the synthesis of nanoscale particles. Moreover, this model confirms the material purity and the crystalline phase. Silver diffractions at 38.2°, 44.5°, 64.3°, and 77.5° belong to the crystal plates (111), (200), (220), and (311), respectively (Anandalakshmi *et al*., 2016). On the other hand, the two weak diffractions at 32.3° and 46.5° represent the presence of silver oxide (Dai *et al*., 2017). The small width of the diffraction pattern at the peak indicates the large crystalline size of the silver nanoparticles. The crystal size of nanoparticles was calculated to be 22 nanometers using the Scherer Equation (Equation C):

$$D = k \times \lambda / \beta \times \cos(\theta) \quad (3)$$

The results of the XRD pattern of Ag-NPs synthesized in this study are consistent with those of Moteriya *et al*. (2017)and Saravanakumar *et al*. (2017).

FTIR Analysis

Characteristics of the nanoparticles were determined using the FTIR spectrum, which was recorded to identify the possible interactions between silver and biologically active molecules involved in the synthesis of nanoparticles. Figure 5 shows the FTIR spectrums of the extract and Ag-NPs samples within the range of 500-4,000 cm^{-1}. Accordingly, the majority of bands are shared in both spectra due to the similar structural components. Yet, there are some differences in the location of peaks due to their dissimilar symmetrical environment and the existing interactions. The observed peak in 3,400-3,500 cm^{-1} belongs to the hydroxyl functional group, which can result from phenolic groups and the absorbed moisture. Besides, the flexural vibration of the hydroxy group shows a peak in 1,620-1,640 cm^{-1}. A small shoulder is observed in both spectra in the range of 1,700 cm^{-1}, which belongs to the C=O carbonyl group vibration. In the extracted sample, the observed vibrations in the range of 1,387, 1,268, and 1,054 cm^{-1} are caused by the stretching vibrations of C-C, C-N, and C-O. These vibrations are displaced slightly and detectable in the Ag-NPs spectrum due to the interaction of the stabilizer with the silver particles. The oxygen-metal (silver in this sample) vibrations show peaks in the range of 500-700 cm^{-1}. The stretching vibrations of the C-

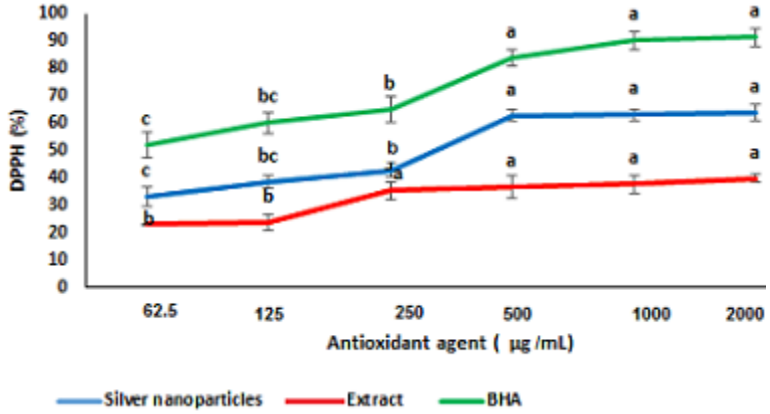

Figure 6. Investigation of DPPH radical inhibition in different concentrations of Ag-NPs synthesized by *V. tricolor*, flower Extract of *V. tricolor* and BHA.

H hydrocarbon structure result in peaks in 2,800-2,900 cm^{-1}. The observed vibration at 2,300 cm^{-1} in the Ag-NPs sample may be attributed to CO_2 absorption during the FTIR sample tableting. As shown in Figure 5, the peaks of phenolic, amine, and carbonyl groups are observed in the spectrum of Ag-NPs, revealing the effect of these functional groups on the synthesis of Ag-NPs.This study was aimed to identify the functional groups and organic compounds in the sample. Bioactive compounds (flavonoids, proteins, exopolysaccharides, polyphenols, and alkaloids) in plant extracts can bind to Ag-NPs via multiple functional groups and, therefore, stabilize Ag-NPs (Siddiqui *et al*., 2017). Consequently, biologically active compounds of the plant can present a satisfactory condition for the synthesis and storage of Ag-NPs without using chemical catalysts or other stabilizers.

Antioxidant Activity

In this study, the effect of DPPH free radical scavenging by synthesized nanoparticles was assessed in comparison with BHA as an industrial antioxidant and positive control and water as a negative control. The results showed that free radical DPPH scavenging activity increased significantly with elevated concentrations of nanoparticles. At a concentration of 62.5 µg mL^{-1}, the free radical scavenging activity is about 33.25%, which increased to about 63.75% at a concentration of 2000 µg mL^{-1} (Figure 6). These results are in line with those of Jagtap *et al*. (2013) on DPPH free radical scavenging using Ag-NPs synthesized from *Rubia tinctorum* and Dauthal *et al*. (2013) on the antioxidant properties of gold and Ag-NPs produced from the apricot fruit extract. Both studies concluded that the antioxidant activity depended on the concentration of Ag-NPs. Most of the antioxidant effects of plant extracts were due to the presence of phenolic compounds such as flavonoids, phenolic acids, etc. Antioxidant activity in plant extracts plays an important role in the peroxide decomposition or free radical neutralization (Ahmed *et al*., 2016).

Antibacterial and Antifungal Activity

As shown in Figure 8, the solution containing Ag-NPs exerted antimicrobial activity against both Gram-positive and Gram-negative bacteria. The results of Duncan's test indicated that the higher the concentration of the plant-derived AgNPs, the larger the diameter of the non-growth halo, with a greater diameter for *E. coli* than

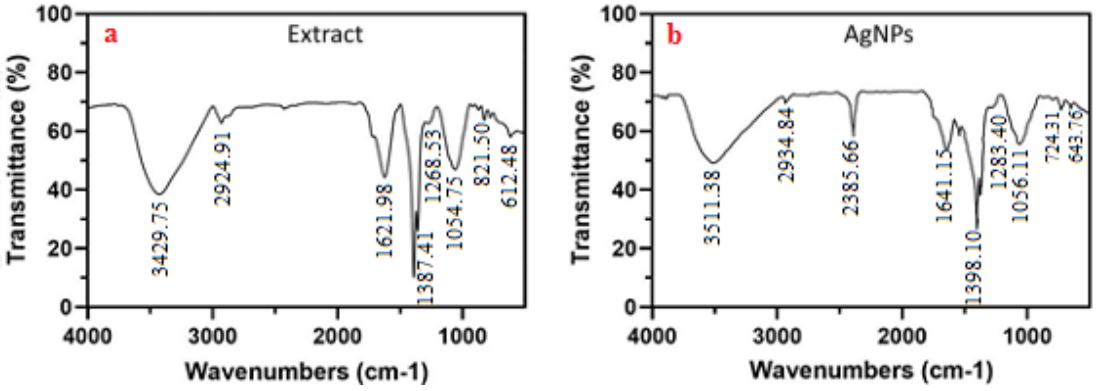

Figure 5. FTIR spectra of vacuum dried powder of: (a) *Viola tricolor* extract, and (b) Ag-NPs.

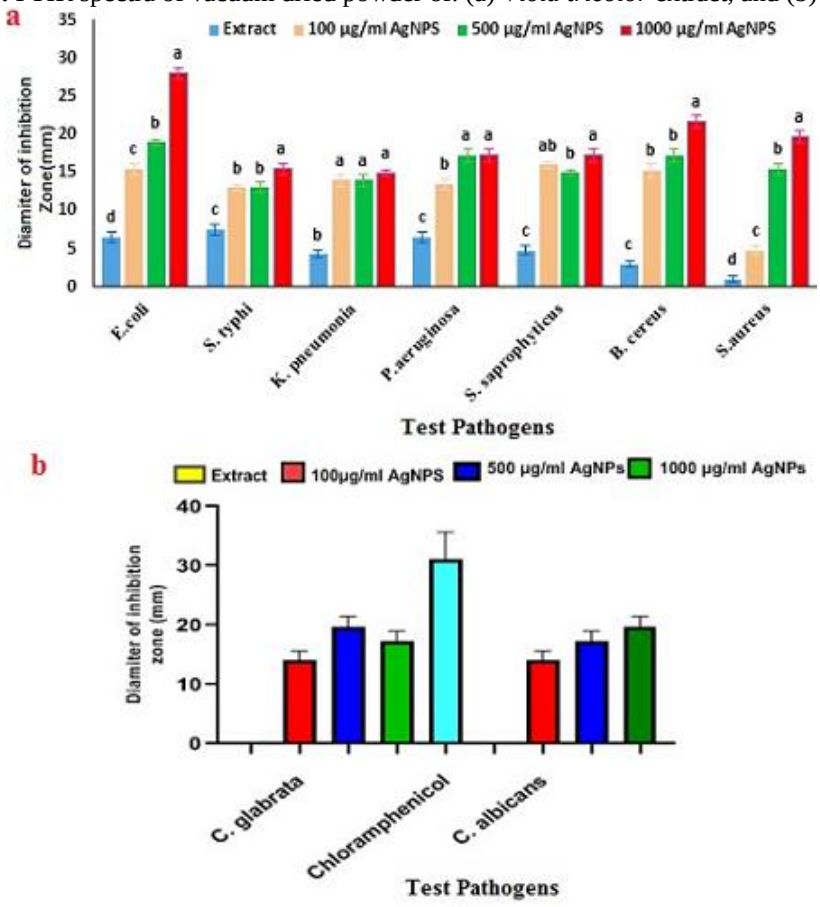

Figure 7. Comparison of different concentrations of Ag-NPs obtained from *Viola tricolor* plant on the diameter of the growth inhibition zone of a bacteria (a) and fungi (b**).**

those of the other studied bacteria at different concentrations of AgNPs. In this study, the maximum non-growth halo diameters in the Ag-NPs were 28, 15.5, 15, 17.25, 21.75, and 19.75 mm for *E. coli*, *S. typhi*, *K. pneumonia*, *P. aeruginosa*, *S. saprophyticus*, *B. cereus*, and *S. aureus*, respectively. Furthermore, there were no significant differences between 100 and 500 µg/mL of Ag-NPs in terms of non-growth halo diameters measured in *S. typhi*, *K. pneumonia*, *S. saprophyticus*, and *B. cereus* (Figure 7-a).

According to Figure 7-b, the largest non-growth halo diameters were observed in *C. albicans* and *C. glabrata* at 1,000 and 500

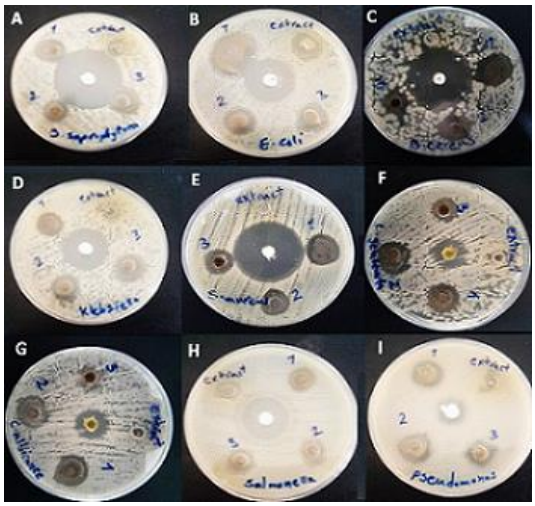

Figure 8. The effect of different concentrations of Ag-NPs and extract *V.tricolor* on bacteria and fungi: (A) *S. saprophyticus*, (B) *E. coli*, (C) *B. cereus* (D) *K. pneumonia*, (E) *S. aureus*, (F) *C. glabrata*, (G) C. *albicans*, (H) *S. typhi*, and (I) *P. aeruginosa.*

μg mL^{-1} of Ag-NPs, respectively, and the extract presented the lowest diameter of the non-growth halo.

The antibacterial and antifungal properties of the *V. tricolor* extract have been reported in many previous studies, but, no study has so far examined the effect of nanoparticles synthesized using the extract of this plant. The mechanism of action of silver relates to their interaction with compounds of the Thiol group in the respiratory enzymes of the bacterial cell. The researchers also attributed the antimicrobial effect of Ag-NPs to the penetration of silver nanoparticles to the bacterial cytoplasmic membrane and its effects on the bacterial respiration chain, RNA, and DNA. Following the silver ion treatment, the cytoplasm membrane shrank and separated from the cell wall. Cellular contents were then released from the cell wall, and the cell wall was degraded (Rashid *et al*., 2016). Studies also suggested that AgNPs could interact with the sulfur-containing proteins and inactivate the amino acids with disulfide bonds. Also, these particles might form pits on the cell wall making it easily permeable and, consequently, leading to bacterial kill(Chen *et al*., 2011).

The results of this study suggested that 1,000 and 500 μg mL^{-1} of Ag-NPs synthesized using *V. tricolor* extract had significant antimicrobial effects against the growth of *S. aureus* and *B. cereus*. However, our data reveal that the greenly synthesized Ag-NPs were significantly more effective against Gram-negative bacteria such as *E. coli*. Saravanakumar *et al*. (2017) also found a high antimicrobial effect of silver hydroxyapatite nanoparticles on both Gram-positive and Gram-negative bacteria.

Ag-NPs cause the death of microbial cells by two mechanisms. A reason for the antimicrobial activity of AgNPs is that silver ions released from Ag-NPs bind to the functional biomolecules of microbial cells, such as oxygen, sulfur, and nitrogen, and lead to the death of bacterial cells (Agarwal *et al*., 2018). Furthermore, Ag-NPs destruct bacterial DNA and lead to bacterial death by producing oxygen free radicals and their binding to bacterial cells. The present results are in agreement with Chand *et al*. (2019), and Keshari, *et al*. (2020) who presented evidence of strong antibacterial properties of Ag-NPs synthesized from plant extracts. In the present study, the synthesized Ag-NPs showed strong antifungal activity against fluconazole-resistant Candida species, which corresponds to that of Nadagouda and Speth (2011).

MIC and MBC Determination

In this study, the antibacterial activity of the AgNPs was investigated by the MIC method, where the bacterial strains were exposed to 125-1,000 μg mL^{-1} of AgNPs. The results showed that AgNPs had antibacterial activity on all studied bacteria such that the lowest and the highest MICs of the extract belonged to B. cereus and K. pneumoniae (Table 1), which is in agreement with Mousavi *et al*. (2018).

The results of MIC and MBC of this type of nanoparticle on seven types of bacteria indicate the growth inhibitory and bactericidal effect of the nanoparticle on

Table 1. The amount of MIC and MBC silver nanoparticles on seven types of bacteria.

MBC (μg mL^{-1}) [a]	MIC (μg mL^{-1})	Bacteria
1000e	900e	*E. coli*
1200c	1100c	*S. saprophyticus*
1600a	1500a	*K. pneumonia*
1000e	900e	*S. thyphi*
900f	800f	*B. cereus*
1400b	1300b	*S. aeureus*
1100d	1000d	*P. aeuroginosa*

[a] Mismatched letters in each column indicate a significant difference at the 5% probability level.

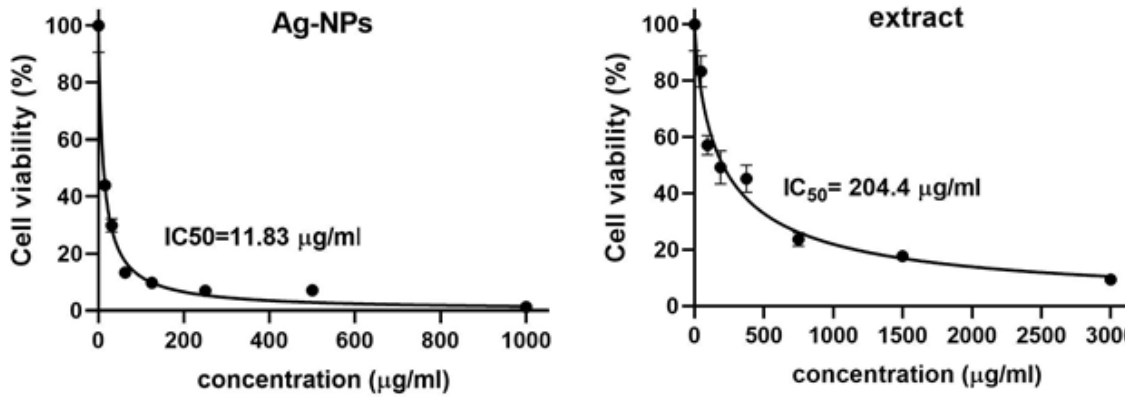

Figure 9. The survival rate of hepatocellular carcinoma cells exposed to different concentrations of Ag-NPs and *V. tricolor* extract.

bacteria in this study. Bacterial growth was observed at a low concentration of nanoparticles, but increasing the concentration of nanoparticles reduced bacterial growth. Therefore, antibacterial effects were directly related to the concentration of biosynthesized silver nanoparticles. The MIC was determined by examining the growth or no growth of bacteria in the culture medium containing different concentrations of nanoparticles. Among the studied bacteria, *Klebsiella pneumonia* and *Bacillus cereus* showed the highest and the lowest resistance, respectively, to biosynthesized nanoparticles. The main mechanism of the antibacterial property of Ag-NPs is the release of silver ions. However, the mechanism of silver ion activity has not yet been fully understood from a molecular microbiology point of view. Some of the principal mechanisms are damage to cell membranes, generation of Reactive Oxygen Species (ROS), and cell invasion by silver ions (or even Ag-NPs due to membrane cavities), followed by damage to ATP products and inhibition of DNA replication (Rashid *et al*., 2016). Cell membrane damage by silver ions has been reported in many studies, which are mainly based on observing large cavities or holes in the bacterial membrane by the SEM analysis. Nano-silver ions may interact with sulfur-containing membrane proteins (e.g. with the thiol protein group in the respiratory chain) and induce physical damage to the membrane. In the present study, the antibacterial effect of Ag-NPs against the studied bacteria may be due to the inability of these microorganisms to replicate themselves and inactivate cellular proteins.

Anticancer Activity Assay

Figure 9 shows the biological ability of AgNPs and the extract on the hepatocellular carcinoma cells obtained by the MTT assay after 24 hours. The measured IC50 of the synthesized AgNPs and the extract were 11.83 and 204.4 μg mL^{-1}, respectively.

According to the figures, the highest survival rate of cancer cells was observed in AgNPs and the extract at a concentration of 0 μg mL^{-1}. Anandan *et al*. (2019) synthesized AgNPs with a size range of 10-20 nm using *Dodonaea viscosa* extract and calculated an IC50 level of 14 μg mL^{-1} for HepG2 hepatocellular carcinoma cells. The toxicity of nanoparticles at effective concentrations on the cancer cells showed a higher potential of nanoparticles in inhibiting the growth of cancer cells. Certainly, biologically produced AgNPs mainly affect the tumor cells. The cytotoxic effect of AgNPs on hepatocellular carcinoma cells suggests that AgNPs may play an essential role in developing potentially useful nanomaterials against various types of cancer. Adebayo *et al*.(2020) showed that AgNPs synthesized using the leaves of *Detarium microcarpum* inhibited pancreatic and cervical cancer cells at IC50s of approximately 84 and 3 μg mL^{-1}, respectively, whereas healthy cells were not affected by these concentrations. The ability of AgNPs to inhibit cancer cells was attributed to the high antioxidant properties of AgNPs synthesized using the leaves of *D. microcarpum* in free radical scavenging. The recent literature indicates that oxidative stress leads to liver and skin cancers due to various factors; therefore, one of the most important mechanisms can be the role of free radicals, which play a key role in cell damage and cancer according to the evidence (Ghavami *et al*., 2009). Oxidative stress in the cell occurs through the activation of lipoxygenase systems and arachidonic acid metabolism along with the production of prostaglandins, which results in lipid peroxidation and producing different freed radicals, causing cell toxicity, mutation, and cancer. Recent studies have shown that the release of radicals or a variety of ROS causes lipid peroxidation in skin cell membranes, which in turn leads to skin cancer and liver damage. In the current study, silver nanoparticles could inhibit free radicals due to their high antioxidant properties, thereby inhibiting cancer cells (Inbathamizh *et al*., 2013). The *V. tricolor* plant extract was reported to have a strong inhibitory effect on the proliferation of cervical cancer cells, which was attributed to the main compound of this plant, i.e. cyclotides, having antitumor and antimicrobial effects.

CONCLUSIONS

The results of this study show the high potential of *V. tricolor* flower extract to reduce metal ions and convert them to nanometric metal atoms. This research shows that Ag-NPs synthesized by the green method are very cost-effective and show high antimicrobial and antioxidant activities. The toxic effect of Ag-NPs on hepatocellular carcinoma cells introduces this nanoparticle as a suitable candidate for the treatment and inhibition of cancer cells. Consequently, further studies are recommended to understand the mechanism of these nanoparticles in the inhibition of cancer cells.

ACKNOWLEDGEMENTS

This research was performed in Razi Herbal Medicines Research Center, Lorestan University of Medical Sciences.

REFERENCES

1. Adebayo, I. A., Arsad, H., Gagman, H. A., Ismail, N. Z. and Samian, M. R. 2020. Inhibitory Effect of Eco-Friendly Naturally Synthesized Silver Nanoparticles from the Leaf Extract of Medicinal *Detarium microcarpum* Plant on Pancreatic and Cervical Cancer Cells. *Asian Pac. J. Cancer Prev*., **21**: 1247–1252.
2. Agarwal, H.; Venkat Kumar, S. and Rajeshkumar, S. 2018. Antidiabetic Effect of Silver Nanoparticles Synthesized Using Lemongrass (*Cymbopogon citratus*) through Conventional Heating and Microwave Irradiation Approach. *J. Microbiol. Biotechnol. Food Sci*., **7**: 371–376.

3. Ahmed, S., Saifullah., Ahmad, M., Swami, B. L. and Ikram, S. 2016. Green Synthesis of Silver Nanoparticles Using *Azadirachta indica* Aqueous Leaf Extract. *J. Radiat Res. Appl. Sci*., **9:** 1–7.
4. Ajitha, B., Reddy, Y. A. K. and Reddy, P. S. 2015. Green Synthesis and Characterization of Silver Nanoparticles Using *Lantana camara* Leaf Extract. *Mater. Sci. Eng. C*., **49**: 373–381.
5. Anandalakshmi, K., Venugobal, J. and Ramasamy, V. 2016. Characterization of Silver Nanoparticles by Green Synthesis Method Using *Pedalium murex* Leaf Extract and Their Antibacterial Activity. *Appl. Nanosci*.,**6:** 399–408.
6. Anandan, M., Poorani, G., Boomi, P., Varunkumar, K., Anand, K., Chuturgoon, A. A., Saravanan, M. and Prabu, H. G. 2019. Green Synthesis of Anisotropic Silver Nanoparticles from the Aqueous Leaf Extract of *Dodonaea viscosa* with Their Antibacterial and Anticancer Activities. *Process Biochem*., **80**: 80–88.
7. Bhakya, S., Muthukrishnan, S., Sukumaran, M. and Muthukumar, M. 2016. Biogenic Synthesis of Silver Nanoparticles and Their Antioxidant and Antibacterial Activity. *Appl. Nanosci*., **6**: 755–766.
8. Bora, K. S. and Sharma, A. 2011. The Genus Artemisia: A Comprehensive Review. *Pharm. Biol*., **49**: 101–109.
9. Chand, K., Abro, M. I., Aftab, U., Shah, A. H., Lakhan, M. N., Cao, D., Mehdi, G. and Mohamed, A. M. A. 2019. Green Synthesis Characterization and Antimicrobial Activity against Staphylococcus aureus of Silver Nanoparticles Using Extracts of Neem, Onion and Tomato. *RSC Adv*., **9:** 17002–17015.
10. Chand, K., Cao, D., Fouad, D. E., Shah, A. H., Dayo, A. Q., Zhu, K., Lakhan, M. N., Mehdi, G. and Dong, S. 2020. Green Synthesis, Characterization and Photocatalytic Application of Silver Nanoparticles Synthesized by Various Plant Extracts. *Arab. J. Chem.*, **13(11):** 8248-8261.
11. Chen, M., Yang, Z., Wu, H., Pan, X., Xie, X. and Wu, C. 2011. Antimicrobial Activity and the Mechanism of Silver Nanoparticle Thermosensitive Gel. *Int. J. Nanomed*., **6**: 2873–2877.
12. Dai, H. Y., Yang, H. M., Jian, X., Liu, X. and Liang, Z. H. 2017. Performance of Ag2O/Ag Electrode as Cathodic Electron Acceptor in Microbial Fuel Cell. *Acta Metallurgica Sinica*, **30**: 1243–1248.
13. Dauthal, P. and Mukhopadhyay, M. 2013. *In-Vitro* Free Radical Scavenging Activity of Biosynthesized Gold and Silver Nanoparticles Using *Prunus armeniaca* (Apricot) Fruit Extract. *J. Nanopart Res*., **15**: 1366.
14. Ebrahimzadeh, M. A., Nabavi, S. M., Nabavi, S. F., Bahramian, F., Bekhradnia, A. R., others. PROVIDE ALL AUTHORS NAMES!! 2010. Antioxidant and Free Radical Scavenging Activity of *H. officinalis* L. var. Angustifolius, *V. odorata, B. hyrcana* and *C. speciosum. Pak. J. Pharm. Sci*., **23**: 29–34.
15. Gan, P. P. and Li, S. F. Y. 2012. Potential of Plant as a Biological Factory to Synthesize Gold and Silver Nanoparticles and Their Applications. *Rev. Environ. Sci. Biotechnol*., **11:** 169–206.
16. Ghavami, S., Hashemi, M., Ande, S. R., Yeganeh, B., Xiao, W., Eshraghi, M., Bus, C. J., Kadkhoda, K., Wiechec, E., Halayko, A. J. and Los, M. 2009. Apoptosis and Cancer: Mutations within *Caspase* Genes. *J. Med. Genet*., **46:** 497–510.
17. Gilavand, F., Saki, R., Mirzaei, S. Z., Esmaeil Lashgarian, H., Karkhane, M. and Marzban, A. 2020. Green Synthesis of Zinc Nanoparticles Using Aqueous Extract of *Magnoliae officinalis* and Assessment of Its Bioactivity Potentials. *Biointerface Res. Appl. Chem*., **11(1)**: 7765-7774
18. Inbathamizh, L., Ponnu, T. M. and Mary, E. J. 2013. *In Vitro* Evaluation of Antioxidant and Anticancer Potential of *Morinda pubescens* Synthesized Silver Nanoparticles. *J. Pharm. Res*., **6:** 32–38.
19. Jagtap, U. B. and Bapat, V. A. 2013. Green Synthesis of Silver Nanoparticles Using *Artocarpus heterophyllus* Lam. Seed Extract and Its Antibacterial Activity. *Ind. Crops Prod*., **46:** 132–137.
20. Keshari, A. K., Srivastava, R., Singh, P., Yadav, V. B. and Nath, G. 2020. Antioxidant and Antibacterial Activity of Silver Nanoparticles Synthesized by *Cestrum nocturnum*. *J. Ayurveda Integr. Med*., **11:** 37–44.
21. Khoshnamvand, M., Huo, C. and Liu, J. 2019. Silver Nanoparticles Synthesized Using *Allium ampeloprasum* L. Leaf Extract: Characterization and Performance

in Catalytic Reduction of 4-Nitrophenol and Antioxidant Activity. *J. Mol. Struct*., **1175**: 90–96.

22. Markus, J., Wang, D., Kim, Y. J., Ahn, S., Mathiyalagan, R., Wang, C., and Yang, D. C. 2017. Biosynthesis, Characterization, and Bioactivities Evaluation of Silver and Gold Nanoparticles Mediated by the Roots of Chinese Herbal Angelica Pubescens Maxim . *Nanoscale Res. Lett. NA*, **12(1):** 46.
23. Moteriya, P. and Chanda, S. 2017. Synthesis and Characterization of Silver Nanoparticles Using *Caesalpinia pulcherrima* Flower Extract and Assessment of Their *in Vitro* Antimicrobial, Antioxidant, Cytotoxic, and Genotoxic Activities. *Artif. Cells Nanomed. Biotechnol*., **45:** 1556–1567.
24. Mousavi, B., Tafvizi, F. and Zaker Bostanabad, S. 2018. Green Synthesis of Silver Nanoparticles Using *Artemisia turcomanica* Leaf Extract and the Study of Anti-Cancer Effect and Apoptosis Induction on Gastric Cancer Cell Line (AGS). *Artif. Cells Nanomed. Biotechnol*., **46:** 499–510.
25. Nadagouda, M. N., Speth, T. F. and Varma, R. S. 2011. Microwave-Assisted Green Synthesis of Silver Nanostructures. *Acc. Chem. Res*., **44**: 469–478.
26. Patra, J. K. and Baek, K. H. 2016. Biosynthesis of Silver Nanoparticles Using Aqueous Extract of Silky Hairs of Corn and Investigation of Its Antibacterial and Anticandidal Synergistic Activity and Antioxidant Potential. *IET Nanobiotechnol*., **10**: 326–333.
27. Poinern, G. E. J., Chapman, P., Shah, M. and Fawcett, D. 2013. Green Biosynthesis of Silver Nanocubes Using the Leaf Extracts from *Eucalyptus macrocarpa*. *Nano Bull*., **2:** 130101.
28. Rashid, M. I., Mujawar, L. H., Rehan, Z. A., Qari, H.; Zeb, J., Almeelbi, T. and Ismail, I. M. I. 2016. One-Step Synthesis of Silver Nanoparticles Using P*hoenix dactylifera* Leaves Extract and Their Enhanced Bactericidal Activity. *J. Mol. Liq*., **223**: 1114–1122.
29. Ravichandran, V., Vasanthi, S., Shalini, S., Shah, S. A. A., Tripathy, M. and Paliwal, N. 2019. Green Synthesis, Characterization, Antibacterial, Antioxidant and Photocatalytic Activity of *Parkia speciosa* Leaves Extract Mediated Silver Nanoparticles. *Results Phys*., **15**: 102565.
30. Ruttkay-Nedecky, B., Krystofova, O., Nejdl, L. and Adam, V. 2017. Nanoparticles Based on Essential Metals and Their Phytotoxicity. *J. Nanobiotechnol*., **15**: 33.
31. Saravanakumar, A., Peng, M. M., Ganesh, M., Jayaprakash, J., Mohankumar, M. and Jang, H. T. 2017. Low-Cost and Eco-Friendly Green Synthesis of Silver Nanoparticles Using *Prunus japonica* (Rosaceae) Leaf Extract and Their Antibacterial, Antioxidant Properties. *Artif. Cells Nanomed. Biotechnol*., **45**: 1165–1171.
32. Siddiqui, M. W., Bansal, V. and Prasad, K. 2017. *Plant Secondary Metabolites. Volume 2: Stimulation, Extraction, and Utilization*. CRC Press Taylor and Francis Group, 318 PP.
33. Tăbăran, A. F., Matea, C. T., Mocan , A., Mihaiu, M., Iancu, C. and Mocan, L. 2020. Silver Nanoparticles for the Therapy of Tuberculosis. *Int. J. Nanomed*., **15**: 2231.
34. Tang, J., Wang, C. K., Pan, X., Yan, H., Zeng, G., Xu, W., He, W., Daly, N. L., Craik, D. J., and Tan, N. 2010. Isolation and Characterization of Cytotoxic Cyclotides from Viola Tricolor. Peptides 31(8): 1434-1440.
35. Yuan, C. G., Huo, C., Gui, B., Liu, P. and Zhang, C. 2017. Green Synthesis of Silver Nanoparticles Using *Chenopodium aristatum* L. Stem Extract and Their Catalytic/Antibacterial Activities. *J. Clust. Sci*., **28**: 1319–1333.

بررسی پتانسیل آنتی اکسیدانی ، ضد میکروبی و ضد سرطانی نانوذرات نقره سنتز شده توسط عصاره بنفشه سه رنگ

ع. حسنوند ، س. سعادتمند، ح. لاری یزدی، و ع. ایرانبخش

چکیده

نانوذرات نقره به سبب خاصیت ضدمیکروبی خود کاربردهای وسیعی در زمینه‌ی پزشکی و داروسازی دارند. در این مطالعه ، نانوذرات نقره با استفاده از عصاره آبی بنفشه سه رنگ به عنوان یک عامل کاهش دهنده و مهارکننده سنتز شدند. ابتدا نانوذرات نقره سنتز گردید و سپس با استفاده از تحلیل های-UV Visible، SEM، TEM، XRD و FTIR وجود نانو ذرات نقره اثبات شد و سپس ویژگی های ضد میکروبی آنها بر اساس حداقل غلظت بازدارندگی (MIC) مورد بررسی قرار گرفت. تجزیه و تحلیل SEM نشان داد که نانوذرات نقره سنتز شده به شکل کروی هستند. هیستوگرام اندازه ذرات نشان داد که متوسط اندازه ذرات 49.45 نانومتر است. یافته های حاصل از طیف FTIR و UV-Vis ، شکل گیری موفقیت آمیز نانوذرات نقره را نشان داد زیرا گروه های عملکردی درگیر در فرایند سنتز و قله های جذب به خوبی توسعه یافته بودند. بعلاوه ، نانوذره نقره حداکثر جذب را در طیف سنجی 420 نانومتر داشت. در مرحله بعد ، نتایج MIC اثرات ضد میکروبی قوی نانوذرات نقره را نشان داد. نتایج MBC سمیت سلولی وابسته به دوز نانوذرات نقره را نشان داد. ذرات نانونقره می توانند اثر مهاری رادیکال های آزاد DDPH را به روشی وابسته به دوز اعمال کنند. نتایج MTT نشان داد که نانوذرات نقره اثر سیتوتوکسیک وابسته به دوز دارند و بقای سلول را به طور قابل توجهی کاهش می دهند. مقادیر IC50 برای نانوذرات نقره و عصاره های نقره به ترتیب 11/83 و 204/4 میکروگرم بر میلی لیتر بود. نتایج این مطالعه نشان داد که اثر سیتوتوکسیک نانو ذرات سنتز شده با روش سبز بر سلولهای سرطان سلولهای کبدی در مقایسه با عصاره قابل توجه است. طبق نتایج این مطالعه ، بیوسنتز نانوذرات نقره با استفاده از عصاره آبی بنفشه سه رنگ تمیز ، ارزان و دارای فعالیت های ضد باکتری ، ضد سرطان و آنتی اکسیدان است که می تواند به عنوان کاندیدای دارویی مورد استفاده قرار گیرد.